Astron. Astrophys. 362, 359–370 (2000)

ASTRONOMY AND ASTROPHYSICS

Time-dependent analytical solutions for MHD surface waves propagating in a compressible plasma

Z.E. Musielak[1,3], **P. Huang**[2], **and P. Ulmschneider**[3]

[1] Department of Physics, University of Texas at Arlington, Arlington, TX 76019, USA
[2] Integraph Corporation, Huntsville, AL 35894-0001, USA
[3] Institut für Theoretische Astrophysik der Universität Heidelberg, Tiergartenstrasse 15, 69121 Heidelberg, Germany

Received 18 January 2000 / Accepted 7 July 2000

Abstract. The propagation of linear MHD surface waves in a compressible plasma with a discontinuous interface in the magnetic field and temperature is considered. The initial perturbation is applied only to a vorticity line, which is located on the RHS of the discontinuity. Two different surface waves exist in this model, one associated with the vorticity line and the other confined to the discontinuity. Time-dependent analytical solutions for the wave velocity perturbations are obtained for both surface waves by applying Laplace transforms. The solutions are used to investigate the effects caused by compressibility on the propagation of these waves. It is shown that the compressibility effects are most important in the vicinity of the vorticity line and at the magnetic interface, and that they affect differently the behavior of the surface waves.

Key words: Magnetohydrodynamics (MHD) – Sun: magnetic fields – Sun: chromosphere – Sun: corona – waves

1. Introduction

The fact that discontinuities in magnetic fields exist in nature and in some laboratory plasma experiments is currently well established (see reviews by Lanzerotti & Southwood 1979; Takahashi & McPherron 1984; Roberts 1991; Solanki 1993; Goossens 1994; Narain & Ulmschneider 1990, 1996). These discontinuities support the existence of magnetohydrodynamic (MHD) surface waves that can locally deposit energy leading to the heating of the background medium. The problem of propagation and dissipation of MHD surface waves has attracted a lot of attention and many important results for laboratory plasmas (e.g., Tataronis & Grossmann 1973; Chen & Hasegawa 1974; Kieras & Tataronis 1982; Tataronis & Lewis 1986) and for magnetized plasmas in solar and stellar atmospheres (e.g., Ionson 1978; Hollweg 1985; Davila 1987; Goossens 1991; Roberts 1991). Under typical conditions occurring in laboratory and atmospheric plasmas, the propagation of surface waves is so complex that it must be investigated by means of numerical simulations (Xiao 1989; Goossens 1994; Ofman et al. 1994; Wu et al. 1996; Huang 1995, 1996; Huang et al. 1999). Because of difficulties in numerical treatments of this type of physical problems (e.g., Ofman et al. 1994; Huang 1996), analytical solutions are required to verify the validity of different numerical codes and to make correct physical interpretation of the obtained numerical results. There is a class of well-known analytical steady-state (Roberts & Webb 1978; Wentzel 1979; Roberts 1981; Cally 1995) and time-dependent (Lee & Roberts 1986) solutions obtained for both discontinuous and finite interfaces embedded in an incompressible plasma. Despite the latter limitation, the solutions have played an important role in our understanding of the behavior of MHD surface waves but, as expected, their applications to the validation of compressible numerical codes have been limited (e.g., Huang 1996). In this paper, we present time-dependent analytical solutions for MHD surface waves propagating in a compressible plasma.

The main motivation for our study was the work by Lee & Roberts (1986), who obtained time-dependent analytical solutions for two different initial value problems. In the first problem, they consider the propagation of MHD surface waves in an incompressible plasma with a discontinuous interface. However, in the second problem, the discontinuity is replaced by a narrow layer in which the physical parameters vary continuously; note that the plasma inside and outside this layer is assumed to be incompressible. Obviously, the analytical solutions to the second problem are of much greater interest than the first one because they allow deriving the decay rate resulting from phase mixing of the existing surface waves. Since the latter may be responsible for the local heating, the result has immediate applications to both laboratory and astrophysical plasmas. Now, the main goal of our paper is to investigate the behavior of linear MHD surface waves propagating in a *compressible* and magnetized plasma with a *discontinuous interface* in the magnetic field and temperature. This simply means that we extend the first initial value problem considered by Lee and Roberts to a compressible plasma. To make direct comparison between their results and ours, we consider the same setting and apply the same initial conditions. As a result, our time-dependent analytical solutions reduce directly to those given by Lee and Roberts when the limit of incompressible plasma is taken into account. We apply Laplace transform method to derive our solutions and

Send offprint requests to: P. Ulmschneider
Correspondence to: ulmschneider@ita.uni-heidelberg.de

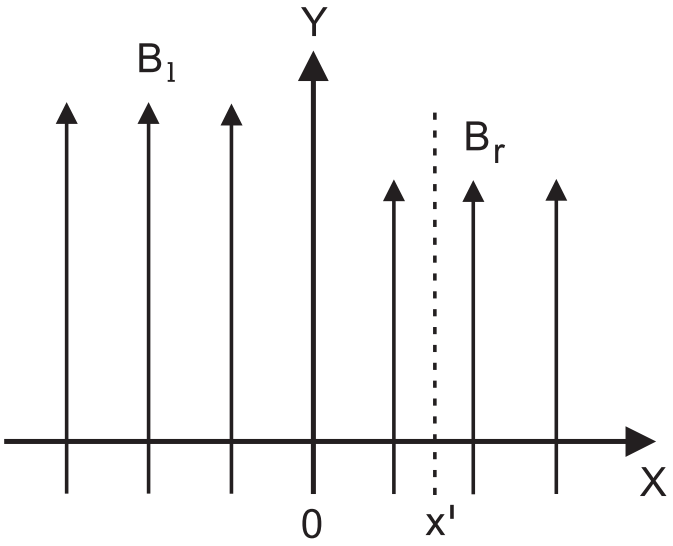

Fig. 1. Single magnetic interface in a compressible medium.

then use them to investigate the effects caused by compressibility on the propagation of MHD surface waves in our model. The obtained analytical solutions can be used to verify the validity of compressible MHD codes and to interpret results of numerical studies of MHD surface waves in compressible plasmas.

For the initial value problem solved in this paper (see Sect. 2), specific initial conditions have been imposed on the background medium at a vorticity line, which is located on the RHS of the magnetic interface (see Sect. 3). The initial value problem has been solved for these initial conditions by using the Laplace transform method (see Sect. 3). The derived solutions have been used to calculate variations of the velocity perturbation in time, for a given location in the background medium, and in space, for a given time interval (see Sect. 4). In the same section, the obtained results are compared to those given by Lee & Roberts (1986) for an incompressible medium. Main conclusions are summarized in the last section of this paper.

2. Physical model and governing equations

A single magnetic interface located in a compressible and magnetized plasma is considered. The background plasma is described by the gas density ρ_0, temperature T_0, pressure p_0, and magnetic field B_0, which allow introducing the sound speed $c_{\rm S} = \sqrt{\gamma p_0/\rho_0}$, with γ being the ratio of specific heats, and the Alfvén velocity $c_{\rm A} = B_0/\sqrt{4\pi\rho_0}$. The interface is assumed to be located along the $y-$axis of a two-dimensional (x, y) cartesian coordinate system, and it separates the background plasma into two regions (see Fig. 1). In the region located on the LHS of the interface $x < 0$ one has $\rho_0 = \rho_l$, $T_0 = T_l$, $p_0 = p_l$, $B_0 = B_l$, $c_{\rm S} = c_{\rm Sl}$ and $c_{\rm A} = c_{\rm Al}$, and in the region on the RHS $x > 0$, $\rho_0 = \rho_r$, $T_0 = T_r$, $p_0 = p_r$, $B_0 = B_r$, $c_{\rm S} = c_{\rm Sr}$ and $c_{\rm A} = c_{\rm Ar}$. To satisfy the pressure balance across the interface

$$p_l + \frac{B_l^2}{8\pi} = p_r + \frac{B_r^2}{8\pi}, \tag{1}$$

the temperature on both sides of the interface is assumed to be different, namely $T_l \neq T_r$, but the gas density is the same $\rho_l = \rho_r = \rho_0$. There are no other gradients in physical parameters either in the x or y-direction, and the background plasma extends to infinity in these two directions.

We assume that wave motions are restricted to the xy-plane, which implies that only *fast* and *slow* MHD body waves are allowed in our model on both sides of the interface and that a surface wave can exist at the interface. Further constraints on our model will be discussed in Sect. 3.1, after the form of initial perturbations is given. It must be also noted that Alfvén waves are formally removed from our model by assuming that no perturbations perpendicular to the xy-plane are taken into account. This physical model is similar to that considered by Lee & Roberts (1986), except that in their case the background medium was assumed to be incompressible; the latter approximation removed the fast MHD wave from their consideration.

The considered physical model is described mathematically by ideal MHD equations. After linearization, the MHD equations can be cast in the form of wave equations written separately for the x and y directions (Roberts 1981)

$$\rho_0 \left(\frac{\partial^2}{\partial t^2} - c_{\rm A}^2 \frac{\partial^2}{\partial y^2}\right) U =$$

$$= \frac{\partial}{\partial x}\left[\rho_0 (c_{\rm S}^2 + c_{\rm A}^2)\frac{\partial U}{\partial x}\right] + \frac{\partial}{\partial x}\left[\rho_0 c_{\rm S}^2 \frac{\partial V}{\partial y}\right], \tag{2}$$

$$\left(\frac{\partial^2}{\partial t^2} - c_{\rm S}^2 \frac{\partial^2}{\partial y^2}\right) V = c_{\rm S}^2 \frac{\partial^2 U}{\partial x \partial y}, \tag{3}$$

where $U(x, y, t)$ and $V(x, y, t)$ represent velocity perturbations in the x and y directions, respectively.

Since the background medium is homogeneous in the y-direction, the velocity perturbations are assumed to be periodic in this direction and given by

$$[U(x, y, t), V(x, y, t)] = [u(x, t)\sin(ky), v(x, t)\cos(ky)]. \tag{4}$$

where k is the wave number. Using these solutions and taking into account the fact that the gas density is the same on both sides of the interface $\rho_l = \rho_r = \rho_0 =$ const, Eqs. (2) and (3) can be written in the following form:

$$\left(\frac{\partial^2}{\partial t^2} + \omega_{\rm A}^2\right) u = \frac{\partial}{\partial x}\left[(c_{\rm S}^2 + c_{\rm A}^2)\frac{\partial u}{\partial x}\right] - \frac{\partial}{\partial x}(\omega_{\rm S} c_{\rm S} v), \tag{5}$$

$$\left(\frac{\partial^2}{\partial t^2} + \omega_{\rm S}^2\right) v = \omega_{\rm S} c_{\rm S} \frac{\partial u}{\partial x}, \tag{6}$$

where

$$\omega_{\rm A,S} = k c_{\rm A,S}. \tag{7}$$

One way to obtain solutions for u and v is to use the Laplace transform method. Defining the Laplace transform of u and v as

$$[\overline{u}(x, s), \overline{v}(x, s)] \equiv \mathcal{L}\{[u(x, t), v(x, t)]\}$$

$$= \int_0^\infty [u(x,t), v(x,t)] e^{-st}\, dt, \tag{8}$$

and taking the Laplace transformation of Eqs. (5) and (6), one obtains

$$(s^2+\omega_{\rm A}^2)\overline{u} = \frac{d}{dx}\left[(c_{\rm S}^2+c_{\rm A}^2)\frac{d\overline{u}}{dx}\right] - \frac{d}{dx}\left(\omega_{\rm S} c_{\rm S}\overline{v}\right) + su(x,0), \tag{9}$$

$$(s^2+\omega_{\rm S}^2)\overline{v} = \omega_{\rm S} c_{\rm S}\frac{d\overline{u}}{dx} + sv(x,0), \tag{10}$$

where $u(x,0)$ and $v(x,0)$ are values of u and v at $t=0$.

Using Eq. (10), one may express $\overline{v}$ in terms of $\overline{u}$ and eliminate it from Eq. (9). This gives

$$\frac{d}{dx}\left[\frac{s^2+\omega_{\rm T}^2}{s^2+\omega_{\rm S}^2}\,(c_{\rm S}^2+c_{\rm A}^2)\frac{d\overline{u}}{dx}\right] - (s^2+\omega_{\rm A}^2)\overline{u} = g(x), \tag{11}$$

where

$$g(x) = \frac{d}{dx}\left[\frac{s\omega_{\rm S}}{s^2+\omega_{\rm S}^2}\, c_{\rm S} v(x,0)\right] - su(x,0), \tag{12}$$

with

$$\omega_{\rm T} = k c_{\rm T} \tag{13}$$

and $c_{\rm T} = c_{\rm S}\, c_{\rm A}/\sqrt{c_{\rm S}^2+c_{\rm A}^2}$ being the cusp speed.

It must be noted that Eq. (11) is very similar to that given by Roberts (1981, see his Eq. 16) who derived his equation by using the Fourier transformation. It is also easy to show that Eq. (11) reduces to that considered by Lee & Roberts (1986, see their Eq. 14) if their initial conditions for u and v are used and the background medium is assumed to be incompressible.

3. Initial value problem and its solutions

3.1. Initial conditions

The derived wave equation for $\overline{u}$ (Eq. 11) can be solved when the initial conditions for $u(x,0)$ and $v(x,0)$ are specified. To investigate the effect of compressibility, we want to compare the results presented in this paper with those previously obtained by Lee & Roberts (1986) for an incompressible medium. To achieve this goal, the initial conditions used here are essentially the same as those considered by Lee and Roberts, who assumed that the initial vorticity in the background medium is non-zero only at the location of the so-called initial vorticity line located on the RHS of the interface (see Fig. 1) and that the initial acceleration of the plasma is zero. Applying these conditions to Eq. (4), one obtains

$$u(x,0) = -\frac{1}{2} Q e^{-k|x-x'|}, \tag{14}$$

$$v(x,0) = \frac{1}{2} Q \frac{(x-x')}{\mid x-x' \mid}\, e^{-k|x-x'|}, \tag{15}$$

where Q represents the perturbation amplitude and x' is the location of the initial vorticity line. These two initial conditions have to be substituted into Eq. (12) in order to obtain the explicit form of the function $g(x)$.

It is clear that the considered initial perturbations have their maxima at the vorticity line and then they quickly decrease with distance from this line. As a result, the generated wave is essentially confined to the vorticity line and it shows properties of a surface wave (see Sect. 4). In this paper, we call this wave the *primary surface wave*. Lee & Roberts called this wave a body wave, but it is clear from its spatial eigenfunction that it is a surface wave; we thank an anonymous referee for pointing this out. Since there is the magnetic interface in the background medium, the imposed initial perturbations are also responsible for the excitation of another surface wave, which propagates along this interface. That wave will be called here the *secondary surface wave*. Thus, in our model only two surface waves are allowed.

3.2. Basic equations

Since the physical conditions on both sides of the interface are different, it is convenient to consider the regions located on the LHS and RHS of the interface separately.

In the region located on the LHS of the magnetic interface $c_{\rm S} = c_{\rm Sl}$, $c_{\rm A} = c_{\rm Al}$ and $c_{\rm T} = c_{\rm Tl}$ are all constant and $x - x'$ is always negative. Introducing $u = u_l$, one can write Eqs. (11) and (12) in the following form:

$$\frac{d^2\overline{u_l}}{dx^2} - m_l^2\overline{u_l} = g_l(x), \tag{16}$$

where

$$m_l^2 = \frac{(s^2+\omega_{\rm Sl}^2)(s^2+\omega_{\rm Al}^2)}{(c_{\rm Sl}^2+c_{\rm Al}^2)(s^2+\omega_{\rm Tl}^2)}, \tag{17}$$

and

$$g_l(x) = \frac{1}{2}\,\frac{Qs}{c_{\rm Sl}^2+c_{\rm Al}^2}\,\frac{s^2}{s^2+\omega_{\rm Tl}^2}\, e^{k(x-x')}. \tag{18}$$

In order to have solutions that describe surface waves, it is required that $m_l^2 > 0$, which means that m_l is neither allowed to be imaginary nor zero (see Roberts 1981).

In the region located on the RHS of the magnetic interface $c_{\rm S} = c_{\rm Sr}$, $c_{\rm A} = c_{\rm Ar}$ and $c_{\rm T} = c_{\rm Tr}$ are all constant. However, the sign of $x - x'$ changes in this region, namely, $x - x'$ it is always negative between the interface and the vorticity line but becomes always positive on the RHS of the vorticity line. To account for this change in sign, two different functions $g_{ri}(x)$, with $i = 1$ and 2, are introduced. Taking $u = u_{ri}$, one may write Eqs. (11) and (12) as

$$\frac{d^2\overline{u_{ri}}}{dx^2} - m_r^2\overline{u_{ri}} = g_{ri}(x), \tag{19}$$

where

$$m_r^2 = \frac{(s^2+\omega_{\rm Sr}^2)(s^2+\omega_{\rm Ar}^2)}{(c_{{\rm S}mr}^2+c_{\rm Ar}^2)(s^2+\omega_{\rm Tr}^2)}, \tag{20}$$

and

$$g_{r1}(x) = \frac{1}{2}\,\frac{Qs}{c_{\rm Sr}^2+c_{\rm Ar}^2}\,\frac{s^2}{s^2+\omega_{\rm Tr}^2}\, e^{k(x-x')}, \tag{21}$$

and

$$g_{r2}(x) = \frac{1}{2}\,\frac{Qs}{c_{\rm Sr}^2+c_{\rm Ar}^2}\,\frac{s^2}{s^2+\omega_{\rm Tr}^2}\,e^{-k(x-x')}. \quad (22)$$

Here it is necessary that $m_r^2 > 0$ and that the functions g_{r1} and g_{r2} are defined only in the regions where $x-x' < 0$ and $x-x' > 0$, respectively. At the location of the vorticity line $x = x'$, we have $g_{r1}(x') = g_{r2}(x')$, which implies that $u_{r1}(x') = u_{r2}(x')$. The continuity of the solution is also required at the location of the interface ($x = 0$), which means that $u_l(0) = u_{r1}(0)$. These conditions will be used later to obtain the solutions to Eqs. (16) and (19).

3.3. General solutions

The standard procedure of finding solutions to inhomogeneous ordinary differential equations with constant coefficients can be applied to Eqs. (16) and (19). The obtained solutions are:

$$\overline{u_l}(x,s) = C_1(s)e^{m_l x} + C_2(s)e^{-m_l x} + C_3(s)e^{k(x-x')}, \quad (23)$$

$$\overline{u_{r1}}(x,s) = C_4(s)e^{m_r x} + C_5(s)e^{-m_r x} + C_6(s)e^{k(x-x')}, \quad (24)$$

and

$$\overline{u_{r2}}(x,s) = C_7(s)e^{m_r x} + C_8(s)e^{-m_r x} + C_9(s)e^{-k(x-x')}, \quad (25)$$

where the terms with the coefficients $C_1(s)$, $C_2(s)$, $C_4(s)$, $C_5(s)$, $C_7(s)$ and $C_8(s)$ represent solutions to the homogeneous parts of Eqs. (16) and (19), and the terms with the coefficients $C_3(s)$, $C_6(s)$ and $C_9(s)$ are the particular solutions. Note that these coefficients are formally the integration constants which are denoted here as functions of s to emphasize the fact that they will provide the time-dependence of the above solutions after their inverse Laplace transforms are found. Since the solutions for $\overline{u_l}$ and $\overline{u_{r2}}$ have to be finite as $x \to -\infty$ and $x \to +\infty$, respectively, one solution in Eq. (23) and one in Eq. (25) are not physically acceptable. To decide which solution has to be dropped, we must first choose the sign of the coefficients m_l and m_r; note that according to Eqs. (16) and (19), the coefficients can be positive or negative but they cannot be imaginary or zero. Hence, we take $m_l > 0$ and $m_r > 0$, which means that two-sided surface waves are allowed (Roberts 1981) and requires that

$$C_2(s) = C_7(s) = 0. \quad (26)$$

Now, the coefficients $C_3(s)$, $C_6(s)$ and $C_9(s)$ can easily be evaluated by substituting the particular solutions to Eqs. (16) and (19). The result is

$$C_3(s) = C_6(s) = C_9(s) = -\frac{Q}{2s}. \quad (27)$$

To determine the remaining four coefficients, namely, $C_1(s)$, $C_4(s)$, $C_5(s)$ and $C_8(s)$, four independent equations are needed. Two of them can be obtained by requiring continuity of the solutions across the magnetic interface $u_l(0) = u_{r1}(0)$ and the initial vorticity line $u_{r1}(x') = u_{r2}(x')$. This gives

$$C_1(s) = C_4(s) + C_5(s), \quad (28)$$

and

$$C_8(s) = C_4(s)e^{2m_r x'} + C_5(s). \quad (29)$$

To obtain two additional equations, Eq. (11) together with the initial conditions given by Eqs. (14) and (15) is integrated across the interface and the vorticity line. After integrating across the interface, one obtains

$$\frac{s^2+\omega_{\rm Ar}^2}{m_r^2}\,\frac{d\overline{u_{r1}}}{dx}\Big|_{x=0} - \frac{s^2+\omega_{\rm Al}^2}{m_l^2}\,\frac{d\overline{u_l}}{dx}\Big|_{x=0}$$

$$= -\frac{1}{2}Q\left(\frac{s\omega_{\rm Sr}}{s^2+\omega_{\rm Sr}^2}c_{\rm Sr} - \frac{s\omega_{\rm Sl}}{s^2+\omega_{\rm Sl}^2}c_{\rm Sl}\right)e^{k(x-x')}\Big|_{x=0}. \quad (30)$$

Using the solutions for $\overline{u_l}$ and $\overline{u_{r1}}$ (see Eqs. 23 and 24), the above equation can be written in the following form:

$$\frac{s^2+\omega_{\rm Ar}^2}{m_r}[C_4(s)-C_5(s)] - \frac{s^2+\omega_{\rm Al}^2}{m_l}C_1(s) = f_1(s)e^{-kx'}, \quad (31)$$

where

$$f_1(s) = \frac{Qk}{2s}\left[\left(\frac{s^2+\omega_{\rm Ar}^2}{m_r^2} - \frac{s^2}{s^2+\omega_{\rm Sr}^2}c_{\rm Sr}^2\right)\right.$$

$$\left. - \left(\frac{s^2+\omega_{\rm Al}^2}{m_l^2} - \frac{s^2}{s^2+\omega_{\rm Sl}^2}c_{\rm Sl}^2\right)\right]. \quad (32)$$

In addition, the integration across the vorticity line yields

$$\frac{s^2+\omega_{\rm Ar}^2}{m_r^2}\left[\frac{d\overline{u_{r2}}}{dx}\Big|_{x=x'} - \frac{d\overline{u_{r1}}}{dx}\Big|_{x=x'}\right]$$

$$= \frac{Q}{2}\frac{s\omega_{\rm Sr}}{s^2+\omega_{\rm Sr}^2}c_{\rm Sr}\left[e^{-k(x-x')} + e^{k(x-x')}\right]\Big|_{x=x'}. \quad (33)$$

Using the solutions given by Eqs. (24) and (25), one gets

$$C_4(s)e^{2m_r x'} - C_5(s) + C_8(s) = 2f_2(s)e^{m_r x'}, \quad (34)$$

where

$$f_2(s) = \frac{Q}{2s}\frac{k}{m_r}\left[1 - \left(\frac{s^2}{s^2+\omega_{\rm Tr}^2}\right)\left(\frac{c_{\rm Sr}^2}{c_{\rm Sr}^2+c_{\rm Ar}^2}\right)\right]. \quad (35)$$

The derived Eqs. (28), (29), (31) and (34) represent four independent relationships that will now be used to obtain the coefficients $C_1(s)$, $C_4(s)$, $C_5(s)$ and $C_8(s)$. By adding Eqs. (29) and (34), the coefficient $C_4(s)$ is easily obtained

$$C_4(s) = f_2(s)\,e^{-m_r x'} \quad (36)$$

The coefficient $C_1(s)$ in Eq. (31) can be eliminated with help of Eq. (28) and Eq. (36) can be used to eliminate the coefficient $C_4(s)$. This gives

$$C_5(s) = \frac{m_l(s^2+\omega_{\rm Ar}^2) - m_r(s^2+\omega_{\rm Al}^2)}{m_l(s^2+\omega_{\rm Ar}^2) + m_r(s^2+\omega_{\rm Al}^2)}f_2(s)e^{-m_r x'}$$

$$- \frac{m_l m_r}{m_l(s^2+\omega_{\rm Ar}^2) + m_r(s^2+\omega_{\rm Al}^2)}\,f_1(s)e^{-kx'}. \quad (37)$$

Having obtained $C_4(s)$ and $C_5(s)$, the two remaining coefficients $C_1(s)$ and $C_8(s)$ can easily be calculated by using Eqs. (28) and (29). Thus, all coefficients of Eqs. (23) through (25) have now been evaluated. An interesting result is that there are only three independent coefficients, namely, $C_4(s)$, $C_5(s)$ and, say (see Eq. 27), $C_6(s)$. This means that the solutions given by Eqs. (23), (24) and (25) can be written as

$$\overline{u_l}(x,s) = C_4(s)e^{m_l x} + C_5(s)e^{m_l x} + C_6(s)e^{k(x-x')}, \quad (38)$$

$$\overline{u_{r1}}(x,s) = C_4(s)e^{m_r x} + C_5(s)e^{-m_r x} + C_6(s)e^{k(x-x')}, \quad (39)$$

and

$$\overline{u_{r2}}(x,s) = C_4(s)e^{-m_r(x-2x')} + C_5(s)e^{-m_r x} + C_6(s)e^{-k(x-x')}. \quad (40)$$

The derived solutions and Eq. (10) can now be used to find the solutions for $\overline{v_l}(x,s)$, $\overline{v_{r1}}(x,s)$ and $\overline{v_{r2}}(x,s)$.

3.4. Dispersion relation

Since the coefficients $C_4(s)$ and $C_5(s)$ depend on the wave number k, we need to evaluate k from the dispersion relation for MHD surface waves; note that k is introduced by Eq. (4) as a result of the periodicity of the solutions in the y-direction. The dispersion relation for these waves is obtained by using the continuity of velocity and total perturbed (gas and magnetic) pressure across the interface (see Wentzel 1979; Roberts 1981) and is given by

$$\omega^2 = \omega_{\rm Al}^2 - \frac{n_l}{n_l + n_r}(\omega_{\rm Al}^2 - \omega_{\rm Ar}^2), \quad (41)$$

where

$$n_{l,r}^2 = \frac{(\omega_{{\rm Sl},r}^2 - \omega^2)(\omega_{{\rm Al},r}^2 - \omega^2)}{(c_{{\rm Sl},r}^2 + c_{{\rm Al},r}^2)(\omega_{{\rm Tl},r}^2 - \omega^2)} \quad (42)$$

is obtained from Eqs. (17) and (18) by taking $s^2 = -\omega^2$ and $m_{l,r}^2 = n_{l,r}^2$. This dispersion relation is transcendental since both n_l and n_r are functions of ω and k. Thus, the value of k for a given wave frequency ω must be evaluated numerically for different values of the plasma β. However, it must be noted that no two-sided surface waves exist if β is small on both sides of the magnetic interface because the wave numbers n_l^2 and n_r^2 cannot both be positive for ω^2 lying between $\omega_{\rm Al}^2$ and $\omega_{\rm Ar}^2$ (Roberts 1981; see also Wentzel 1979, for discussion of one-sided surface waves).

3.5. Solutions for a compressible medium

After discussing the dispersion relation for surface waves and introducing the wave numbers n_l and n_r, we may now calculate the inverse Laplace transforms for $\overline{u}$ and $\overline{v}$ by evaluating the following integrals

$$[u_l(x,t), u_{r1}(x,t), u_{r2}(x,t)]$$

$$\equiv \mathcal{L}^{-1}\{[\overline{u_l}(x,s), \overline{u_{r1}}(x,s), \overline{u_{r2}}(x,s)]\}$$

$$= \frac{1}{2\pi i}\int_C [\overline{u_l}(x,s), \overline{u_{r1}}(x,s), \overline{u_{r2}}(x,s)]\, e^{st}\, ds, \quad (43)$$

where C is the path of the integration in the complex plane and s is a complex quantity. Obviously, similar integrals must be evaluated to find $v_l(x,t)$, $v_{r1}(x,t)$ and $v_{r2}(x,t)$.

Detailed evaluation of the integrals given by Eqs. (44), (45) and (46) can be found in the Appendix, however, here we present only the final results. The inverse Laplace transforms of $u_l(x,t)$, $u_{r1}(x,t)$ and $u_{r2}(x,t)$ can be written as

$$u_l(x,t) = \frac{Q}{2}\left[(\alpha_1 - \alpha_0)\,\cos(\omega_{\rm Tr}t) + (\alpha_3 - \alpha_2)\,\cos(\omega t)\,\right] e^{n_l x}e^{-n_r x'}\,, \quad (44)$$

$$u_{r1}(x,t) = \frac{Q}{2}\left[(\alpha_1 - \alpha_0\, e^{2n_r x})\,\cos(\omega_{\rm Tr}t) + (\alpha_3 - \alpha_2)\,\cos(\omega t)\,\right] e^{-n_r(x+x')}\,, \quad (45)$$

and

$$u_{r2}(x,t) = \frac{Q}{2}\left[(\alpha_1 - \alpha_0\, e^{2n_r x'})\,\cos(\omega_{\rm Tr}t) + (\alpha_3 - \alpha_2)\,\cos(\omega t)\,\right] e^{-n_r(x+x')}\,, \quad (46)$$

where

$$\alpha_0 = \frac{k}{n_r}\frac{c_{\rm Sr}^2}{c_{\rm Sr}^2 + c_{\rm Ar}^2}\,, \quad (47)$$

$$\alpha_1 = \frac{n_l(\omega_{\rm Ar}^2 - \omega_{\rm Tr}^2) - n_r(\omega_{\rm Al}^2 - \omega_{\rm Tr}^2)}{(n_l + n_r)\,(\omega_{\rm Tr}^2 - \omega^2)}\,\alpha_0\,, \quad (48)$$

$$\alpha_2 = \frac{n_l(\omega_{\rm Ar}^2 - \omega^2) - n_r(\omega_{\rm Al}^2 - \omega^2)}{(n_l + n_r)\,(\omega_{\rm Tr}^2 - \omega^2)}\,\alpha_0\,, \quad (49)$$

and

$$\alpha_3 = \frac{k}{n_r}\left(\frac{n_r}{n_l + n_r}\right)\left[\left(1 - \frac{n_r}{n_l}\right)\left(\frac{\omega_{\rm Al}^2 - \omega^2}{\omega^2}\right) + \left(\frac{n_l n_r c_{\rm Sr}^2}{\omega_{\rm Sr^2} - \omega^2} - \frac{n_l n_r c_{\rm Sl}^2}{\omega_{\rm Sl^2} - \omega^2}\right)\right]\,. \quad (50)$$

According to these solutions, there is a superposition of two different normal modes at each point in the background medium. One mode can be identified as the primary surface wave and is described by the terms with $\cos(\omega_{\rm Tr}t)$ in the above equations. This wave propagates freely in the y-direction with the characteristic frequency $\omega_{\rm Tr}$, and its maximum amplitude is at the location of the vorticity line, where the initial velocity perturbation is applied. The other mode can be identified as the secondary surface wave and its behavior is described by the terms with $\cos(\omega t)$ in the above solutions. This wave owes its existence to the presence of the magnetic interface in the background medium and, therefore, its maximum intensity is at the

location of this discontinuity. The propagation of this wave in the y-direction is free and its characteristic frequency is ω. A detailed discussion of the behavior of both MHD surface waves in a compressible plasma is given in Sect. 4.

Finally, it must be noted that similar calculations must be performed to evaluate the inverse Laplace transforms of $v_l(x,t)$, $v_{r1}(x,t)$ and $v_{r2}(x,t)$ - see Eq. (8). However, in this paper, we restrict our attention to the velocity perturbations $u_l(x,t)$, $u_{r1}(x,t)$ and $u_{r2}(x,t)$.

3.6. Special case: incompressible medium

Having obtained the general solutions for the case of a compressible medium, we now take the limit of an incompressible medium $c_{\rm Sl} \to \infty$ and $c_{\rm Sr} \to \infty$, and obtain $n_l = k$, $n_r = k$, $\alpha_0 = 1$, $\alpha_1 = 1$, $\alpha_2 = 1$, and $\alpha_3 = 0$. Applying these results to Eqs. (44), (45) and (46), we get

$$u_l(x,t) = -\frac{Q}{2}\cos(\omega t)\, e^{k(x-x')}, \tag{51}$$

$$u_{r1}(x,t) = -\frac{Q}{2}\left[2\sinh(kx)\, \cos(\omega_{\rm Ar} t)\, e^{-kx'} + \cos(\omega t)\, e^{-k(x+x')}\right]. \tag{52}$$

and

$$u_{r2}(x,t) = -\frac{Q}{2}\left[2\sinh(kx')\, \cos(\omega_{\rm Ar} t)\, e^{-kx} + \cos(\omega t)\, e^{-k(x+x')}\right], \tag{53}$$

where

$$\omega^2 = \frac{1}{2}(\omega_{\rm Al}^2 + \omega_{\rm Ar}^2). \tag{54}$$

The derived solutions for the case of an incompressible medium are identical to those obtained by Lee & Roberts (1986). It is seen that the primary surface wave with the characteristic frequency $\omega_{\rm Ar}$ is present in the background medium and its maximum amplitude is at the vorticity line (see Sect. 4, for more details). In addition, there is the secondary surface wave with the characteristic frequency ω and this wave is confined to the magnetic interface. An interesting result is that the primary surface wave is present in the background medium only on the RHS of the magnetic interface. The results obtained for a compressible medium showed that this wave was also present on the LHS of the discontinuity (see Eq. 44). This is one of main differences (see Sect. 4, for more detailed discussion) between the wave behavior in compressible and incompressible plasmas.

4. Effects of compressibility

4.1. Analytical results: individual surface waves

To discuss the effects of compressibility, we need to plot the derived solutions as a function of time, distance and the plasma

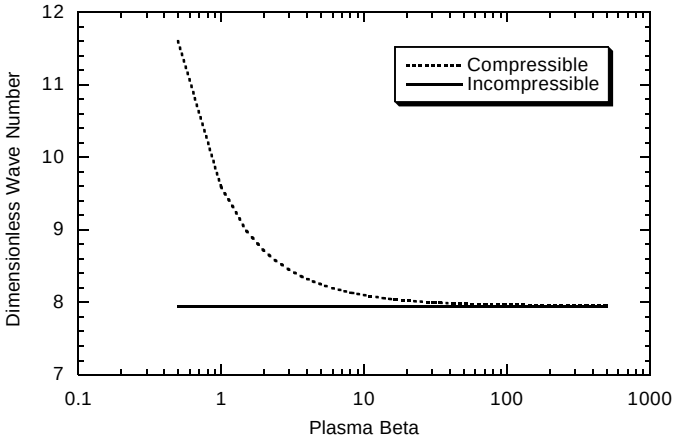

Fig. 2. Wave number $[k]$ is plotted as a function of the plasma β on the LHS of the magnetic interface. The value of $[k]$ obtained for the case of an incompressible medium is also plotted for comparison.

β. To compare different solutions, it is convenient to dimensionalize all physical quantities in the derived analytical solutions by introducing a characteristic time, $t_0 = P$, where $P = 2\pi/\omega$ is the wave period, and a characteristic length $l_0 = c_{\rm Al}P$. We begin with the obtained dispersion relation and show the dependence of the wave number k on the plasma β. Using t_0 and l_0, we write Eq. (41) in the following form:

$$[k]^2 = \frac{(2\pi)^2}{1 - \frac{[n_l]}{[n_l]+[n_r]}(1-\sigma^2)}, \tag{55}$$

where all quantities in square-brackets are dimensionless and $[k] = kl_0$, $[\omega] = \omega t_0 = 2\pi$,

$$[n_l]^2 = \frac{([k]^2[c_{\rm Sl}]^2 - 4\pi^2)\,([k]^2 - 4\pi^2)}{([c_{\rm Sl}]^2 + 1)\,([k]^2[c_{\rm Tl}]^2 - 4\pi^2)}, \tag{56}$$

and

$$[n_r]^2 = \frac{([k]^2[c_{\rm Sr}]^2 - 4\pi^2)\,([k]^2\sigma^2 - 4\pi^2)}{([c_{\rm Sr}]^2 + [c_{\rm Ar}]^2)\,([k]^2[c_{\rm Tr}]^2 - 4\pi^2)}, \tag{57}$$

with $[c_{{\rm Sl},r}]^2 = \gamma\beta_{l,r}/2$, where $\beta_{l,r}$ is the plasma β on the LHS and RHS of the interface, respectively, and $[c_{\rm Ar}]^2 = B_r^2/B_l^2 \equiv \sigma^2$. In addition, we have $[c_{\rm Tl}]^2 = [c_{\rm Sl}]^2/(1+[c_{\rm Sl}]^2)$ and $[c_{\rm Tr}]^2 = \sigma^2[c_{\rm Sr}]^2/(\sigma^2+[c_{\rm Sl}]^2)$. Using the pressure balance across the interface (Eq. 1), we express β_r in terms of β_l and σ, and obtain $\beta_r = \beta_l + 1 - \sigma^2$. Finally, defining $\beta \equiv \beta_l$ and taking $\sigma = 0.5$, we compute $[k]$ as a function of the plasma β. The results are plotted in Fig. 2 and compared to the value of $[k]$ obtained in the case of an incompressible medium; note that in the latter case $[k]$ does not depend on β because it is obtained in the limit of $\beta \to \infty$. The results presented in Fig. 2 clearly show that $[k]$ calculated for the case of a compressible medium rapidly increases as β approaches 0.5. Therefore, we limit all our calculations to $\beta \geq 0.5$.

We now use t_0 and l_0 to dimensionalize the solutions given by Eqs. (44), (45) and (46). Since the form of these solutions does not change significantly when they are dimensionalized, we will not rewrite them again here but instead

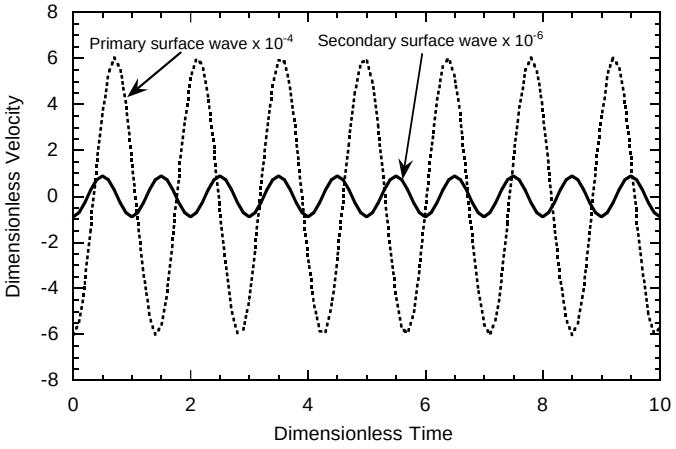

Fig. 3. Wave velocities for the primary (dotted line) and secondary (solid line) surface wave are plotted as a function of time at the vorticity line located at $[x] = [x'] = 0.5$. The results were obtained by taking $\beta = 1$.

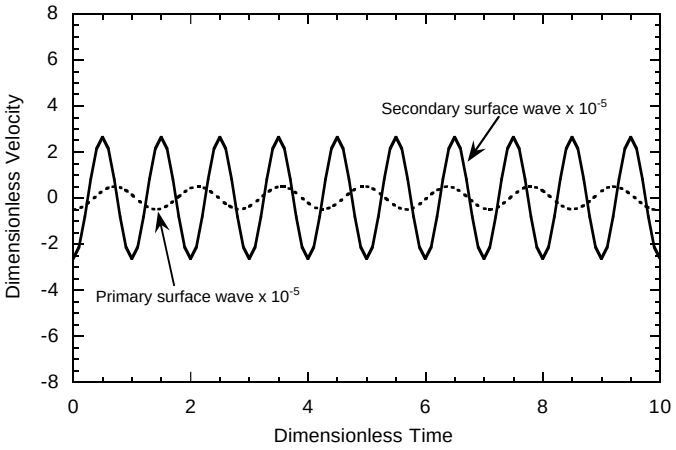

Fig. 4. The same as Fig. 3 but at the location of the magnetic interface ($[x] = 0.0$).

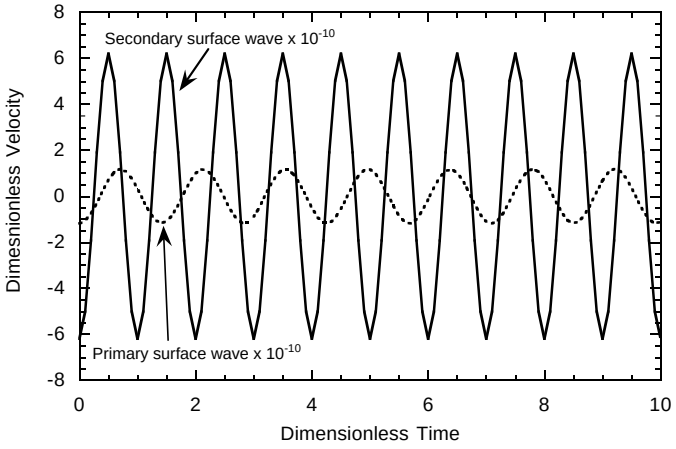

Fig. 5. The same as Fig. 3 but at $[x] = -0.5$.

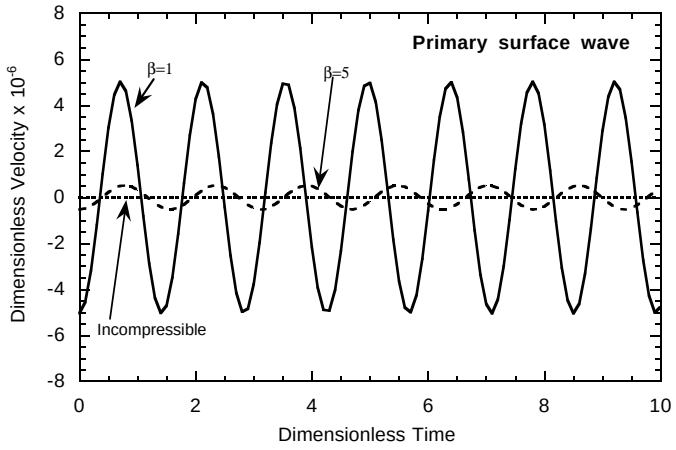

Fig. 6. Wave velocities for the primary surface wave propagating at the location of the magnetic interface ($[x] = 0$) are plotted as a function of time for $\beta = 1$ and 5, and for the case of an incompressible medium.

introduce $[\omega_{\rm Al}] = [k]$, $[\omega_{\rm Ar}] = \sigma[k]$, $[\omega_{{\rm Sl},r}] = [k][c_{{\rm Sl},r}]$, $[\omega_{{\rm Tl},r}] = [k][c_{{\rm Tl},r}]$, $[Q] = Q/c_{\rm Al}$, $[x] = x/l_0$, $[x'] = x'/l_0$, and $[t] = t/t_0$. The dimensionalized solutions are plotted as a function of time for several different locations with respect to the vorticity line (see Figs. 3, 4 and 5), as a function of space for different instants of time (see Fig. 6), and as a function of space for a fixed time and for different values of the plasma β (see Fig. 7). To understand the results presented in these figures, one needs to keep in mind that the initial wave motion is originally generated at the vorticity line ($[x] = [x'] = 0.5$) and that it freely propagates in the y-direction (see Eqs. 4 and 5). This initial perturbation affects the magnetic field lines on both sides of the vorticity line and is responsible for the excitation of both the primary and secondary surface waves. Hence, in the following we discuss the wave behavior on different sides of the vorticity line and interface.

The magnetic field on both sides of the interface responds to the wave excited at the vorticity line by supporting wave motions outside this line. According to the derived solutions, there are two normal modes: the primary and secondary surface waves. The results presented in Figs. 3, 4 and 5 show that both waves are always periodic in time and that they have different amplitudes at different locations in the background medium. The amplitude of the primary surface wave exceeds that of the secondary surface wave at the vorticity line (see Fig. 3), however, at the interface ($[x] = 0$) the amplitude of the secondary surface wave is always larger (see Fig. 4). According to Fig. 5, the primary surface wave is also present on the LHS ($[x] = -0.5$) of the interface but its amplitude is lower than that of the secondary surface wave. It can also be seen that the secondary surface wave propagates with the dimensionless frequency [ω] = 1 (see Fig. 3) and that the dimensionless frequency of the primary surface wave is [$\omega_{\rm Tr}$] on both sides of the interface (compare Figs. 3 and 5).

The dependence of the primary and secondary surface waves on the plasma β at the location of the magnetic interface is shown in Figs. 6 and 7, respectively. The amplitude of the primary surface wave increases with decreasing β and in the limit of an incompressible medium the wave is not present anymore (see Fig. 6). It is also seen that the frequency of the primary surface wave increases when β decreases; this can be explained by the

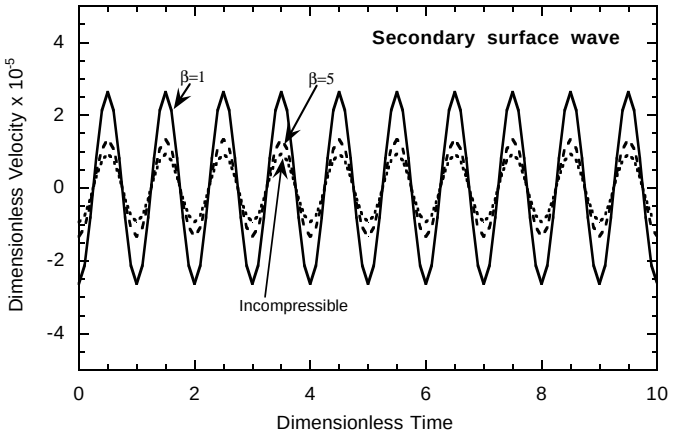

Fig. 7. The same as Fig. 6 but for the secondary surface wave.

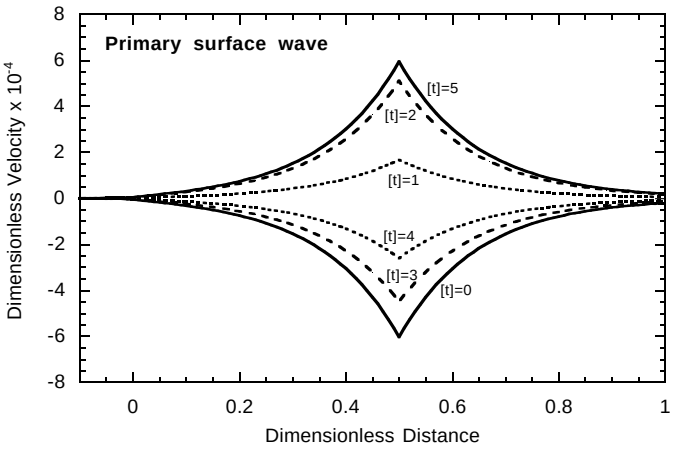

Fig. 8. Wave velocities for the primary surface wave are plotted as a function of distance for the dimensionless time $[t] = 1$, 2, 3, 4 and 5. Note that the wave has the maximum amplitude at the location of the vorticity line ($[x] = [x'] = 0.5$). The calculations were performed with $\beta = 1$.

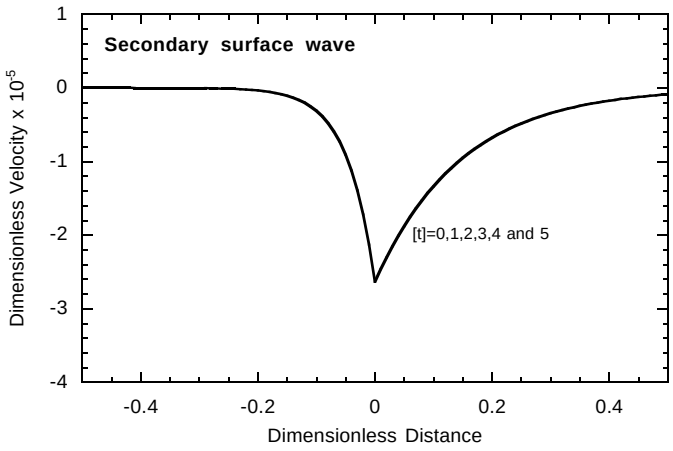

Fig. 9. Wave velocities for the secondary surface wave are plotted as a function of distance for the dimensionless time $[t] = 1$, 2, 3, 4 and 5. Note that the wave has the maximum amplitude at the location of the interface ($[x] = 0.0$). The calculations were performed with $\beta = 1$.

fact that $[\omega_{\rm Tr}] = [k][c_{\rm Tr}]$, which means that $[\omega_{\rm Tr}]$ increases when $[k]$ increases for the compressible medium (see Fig. 2). Now, the effects caused by compressibility on the behavior of the secondary surface wave are much smaller and only the wave amplitude is affected (see Fig. 7). The presented result show that the secondary surface wave is always present in the background medium and that only small differences in the wave amplitude can be seen when the compressible and incompressible cases are compared.

The decrease of the amplitude of the primary surface wave with distance from the vorticity line is shown in Fig. 8. The presented results are given for several chosen instants of time. As expected, the maximum wave amplitude occurs at the vorticity line, where the wave is originally generated. The amplitude rapidly decreases with distance from the vorticity line and is much smaller at the interface ($[x] = 0$) than at $[x] = 1$. This asymmetry in the wave behavior can be explained by the fact that the magnetic field on the LHS of the interface is two times stronger than that on the RHS ($\sigma = 0.5$). In addition, it is seen that the dimensionless period of this surface wave is different than unity (compare, for example, the results obtained for $[t] = 2$ and 3) and, as a result, the wave amplitude is different for different values of $[t]$. These differences are not seen in Fig. 9, which shows similar results but for the secondary surface wave. Since the dimensionless period of this surface wave is $[P] = [t] = 1$, the pattern of the wave amplitude repeats itself for every chosen instant of time. The maximum amplitude of this wave occurs at the magnetic interface and rapidly decreases away from it. There is some asymmetry in the wave amplitude on both sides of the interface, namely, the amplitude on the RHS of the interface is always larger, and decreases slower, than the corresponding wave amplitude on the RHS of the interface. Again, the difference in the magnetic field strength on both sides of the interface is responsible for this wave behavior.

4.2. Analytical results: superposition of surface waves

In the previous subsection, we treated both surface waves separately and concentrated on the effects caused by compressibility on the behavior of these waves. However, our analytical solutions show that the existing wave motions should be treated as a superposition of both waves. To address this problem, we plot the wave velocity as a function of distance for the general solutions given by Eqs. (44) through (50), and for different values of plasma β (see Figs. 10 and 11). It must be kept in mind that the results presented in these figures are obtained for one specific instant of time, namely, $[t] = 5$. The results show that the so-called *compressible* cases always reduce to the *incompressible* case when the plasma β is increased from 1 to 20. The solution obtained with $\beta = 20$ differs only very slightly from the incompressible case, which means that the wave motions considered in a medium with $\beta \geq 20$ can be approximated by the incompressible solution. The obtained results also show that the wave velocity is positive when the plasma $\beta \leq 2.5$ and negative for larger values of β. Obviously, this is true only for the chosen

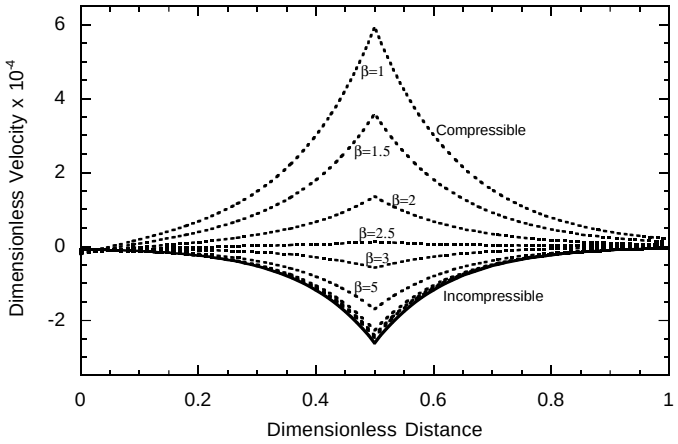

Fig. 10. Wave velocity is plotted as a function of distance from the interface located at $[x] = 0$ for different values of plasma β. The curve labelled *compressible* corresponds to $\beta = 1$ and the curve labelled *incompressible* represents the case when $\beta \to \infty$. Two dotted-lines located near the solid line represent the results obtained with $\beta = 10$ and 20. All results shown in this figure were obtained for $[t] = 5$.

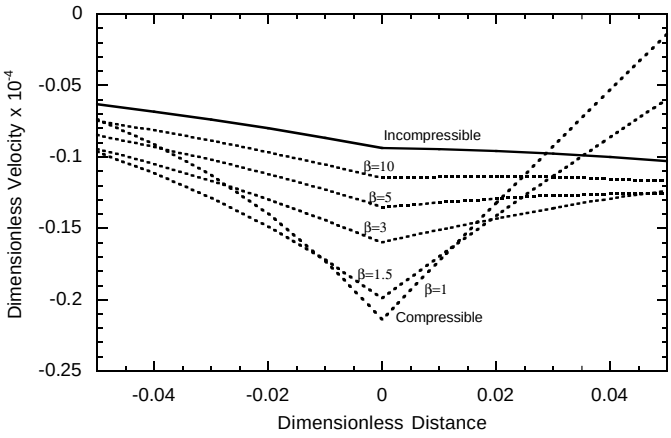

Fig. 11. Dimensionless wave velocity is plotted as a function of dimensionless distance in the vicinity of the interface located at $x = 0$ for different values of plasma β. The curve labelled *compressible* corresponds to $\beta \leq 1$ and the curve labelled *incompressible* formally represents the case when $\beta \to \infty$. All results shown in this figure were obtained for $[t] = 5$.

instant of time as the wave velocity oscillates in time (see, for example, Fig. 8).

The results presented in Fig. 10 show the behavior of the superposition of both surface waves in the vicinity of the vorticity line. Based on the results discussed in Sect. 4.1, it is obvious that the primary surface wave dominates in the wave behavior in this region of the background medium. As expected, the maximum of the wave amplitude is at the vorticity line. The wave amplitude also depends on the plasma β and, for the chosen time $[t] = 5$, the largest wave amplitude is obtained for the compressible case with $\beta = 1$. It is also seen that the solutions approach the incompressible one when the distance from the vorticity line is increased, and that the wave behavior on the RHS and LHS of the vorticity line is always different. This asymmetry in the wave behavior is caused by the presence of the secondary surface wave at the interface and in its vicinity. Since the secondary surface wave dominates in the wave behavior at and near the interface, the solutions shown in Fig. 11 represent mainly the behavior of this wave.

By comparing the results presented in Figs. 10 and 11, one sees that compressibility affects the primary and secondary surface waves differently. This becomes especially obvious when the solutions for these two waves obtained for $\beta \leq 1.5$ are compared. It is also seen that the behavior of the secondary surface wave on both sides of the interface is not the same and the effects are more prominent for a low-β plasma. The behavior of this wave at the interface can be explained by the fact that the physical conditions on its both sides are different and, as a result, the wave velocity and the total (gas and magnetic) wave pressure must be adjusted to satisfy the requirement of continuity across the interface. Thus, the presence of the interface in the background medium strongly affects the wave behavior. Based on the presented results, we may conclude that the compressibility effects are most important in the vicinity of the vorticity line and the interface. Additional discussion of these effects is given by Huang (1995, 1996) and Huang et al. (1999) who computed numerically the entire wave velocity field and compared it to that obtained from analytical calculations.

5. Conclusions

We have solved analytically the initial value problem for linear MHD surface waves propagating in a compressible medium with a single magnetic interface and a vorticity line. The initial perturbations are applied at the vorticity line and the resulting wave motions are described by the time-dependent analytical solutions obtained by using Laplace transforms. In the limit of an incompressible medium, the derived analytical solutions reduce to those previously obtained by Lee & Roberts (1986).

We have used our analytical solutions to show that the wave velocity field can be represented by a superposition of the primary and secondary surface waves that exist everywhere in the background medium. The primary surface wave dominates in the wave motions at and near the vorticity line, while the intensity of the secondary surface wave is the highest at the magnetic interface and in its vicinity. The dimensionless frequency of the secondary surface wave is $[\omega] = 1$. However, the primary surface wave propagates with the dimensionless frequency $[\omega_{\rm Tr}]$ on both sides of the magnetic interface.

Our results demonstrate that the compressibility effects are most important in the vicinity of the vorticity line and the magnetic interface, and that they affect differently the behavior of both MHD surface waves. It is also shown that the so-called compressible cases (with a plasma $\beta \leq 5$) reduce to the incompressible case when the plasma β is increased to 20. The solution obtained with $\beta = 20$ differs only very slightly from the incompressible case, which means that the wave motions considered in a medium with $\beta \geq 20$ can be approximated by the incompressible solution.

Finally, we suggest that the derived analytical solutions can be used to test the validity of some numerical codes developed to study the propagation of MHD waves in a medium with highly structured magnetic fields.

Acknowledgements. We thank an anonymous referee for helpful comments and suggestions. This work was supported by NATO under grant CRG-910058 (P.U. and Z.E.M.) and by the Alexander von Humboldt Foundation (Z.E.M.)

Appendix A: evaluation of inverse Laplace transforms

To evaluate the inverse Laplace transform of $u_l(x,t)$, we combine Eqs. (43) and (38) to obtain

$$u_l(x,t) = \frac{1}{2\pi i}\left[\int_C C_4(s)e^{m_l x}e^{st}ds + \int_C C_5(s)e^{m_l x}e^{st}ds + \frac{1}{2\pi i}\int_C C_6(s)e^{k(x-x')}e^{st}ds\right], \quad (A.1)$$

where C is the path of the integration in the complex plane and s is a complex quantity.

We begin with the first integral and use Eqs. (35) and (36) to write it in the following form:

$$\frac{1}{2\pi i}\int_C C_4(s)e^{m_l x}e^{st}ds = I_1 + I_2, \quad (A.2)$$

where

$$I_1 = \frac{1}{2\pi i}\int_C F_1(s)ds, \quad (A.3)$$

with

$$F_1(s) = \frac{1}{s}\frac{k}{m_r}e^{-m_r x'}e^{m_l x}e^{st}, \quad (A.4)$$

and

$$I_2 = -\frac{1}{2\pi i}\int_C F_2(s)ds, \quad (A.5)$$

with

$$F_2(s) = \left(\frac{s^2}{s^2+\omega_{\rm Tr}^2}\right)\left(\frac{c_{\rm Sr}^2}{c_{\rm Sr}^2+c_{\rm Ar}^2}\right)F_1(s). \quad (A.6)$$

Since we consider two-sided MHD surface waves, m_r must always be positive (see the main text), which means that $F_1(s)$ has only one pole at $s=0$. By calculating the residue of $F_1(s)$ at $s=0$ and noting that $m_l = k$ and $m_r = k$ for $s=0$, we obtain

$$I_1 = \frac{Q}{2}e^{k(x-x')}. \quad (A.7)$$

To evaluate the integral I_2, we again take $m_r > 0$ and find that $F_2(s)$ has two poles at $s = \pm i\omega_{\rm Tr}$. By applying the limit $s \to \pm i\omega_{\rm Tr}$ to m_r, we find that $m_r \to \infty$ and, as a result, $I_2 = 0$ and the solutions given by Eqs. (38), (39) and (40) become unphysical. Since in our approach neither $m_{l,r} = 0$ nor $m_{l,r} = \infty$ are allowed, we need to determine $m_{l,r}$ before the integral I_2 is formally evaluated. The results obtained for the integral I_1 demonstrate that $m_{l,r} = k$ if $s = 0$. In addition, our analysis of poles for the second integral in Eq. (A1) shows that $m_{l,r} = n_{l,r}$ if $s = \pm i\omega$ (see Eq. A19, and also Eqs. 41 and 42 in the main text). It can easily be shown that these are the only cases when the physically acceptable solutions are obtained. Because we consider here a compressible medium, we evaluate the integral I_2 by taking $m_{l,r} = n_{l,r}$. This allows us to write

$$F_2(s) = \frac{k}{n_r}\left(\frac{s}{s^2+\omega_{\rm Tr}^2}\right)\left(\frac{c_{\rm Sr}^2}{c_{\rm Sr}^2+c_{\rm Ar}^2}\right)e^{-n_r x'}e^{n_l x}e^{st}, \quad (A.8)$$

and calculate the residue of $F_2(s)$ at $s = \pm i\omega_{\rm Tr}$

$$I_2 = -\frac{Q}{2}\frac{k}{n_r}\left(\frac{c_{\rm Sr}^2}{c_{\rm Sr}^2+c_{\rm Ar}^2}\right)e^{-n_r x'}e^{n_l x}\cos(\omega_{\rm Tr}t). \quad (A.9)$$

As the next step, we evaluate the second integral in Eq. (A1). By using Eqs. (32), (35) and (37), we write this integral in the following form:

$$\frac{1}{2\pi i}\int_C C_5(s)e^{m_l x}e^{st}ds = I_3 + I_4 + I_5 + I_6, \quad (A.10)$$

where

$$I_3 = \frac{1}{2\pi i}\int_C F_3(s)ds, \quad (A.11)$$

with

$$F_3(s) = \frac{\left[m_l(s^2+\omega_{\rm Ar}^2) - m_r(s^2+\omega_{\rm Al}^2)\right]F_1(s)}{(m_l+m_r)\left[s^2+\omega_{\rm Al}^2 - \frac{m_l}{m_l+m_r}(\omega_{\rm Al}^2-\omega_{\rm Ar}^2)\right]} \quad (A.12)$$

$$I_4 = -\frac{1}{2\pi i}\int_C F_4(s)ds, \quad (A.13)$$

with

$$F_4(s) = \frac{\left[m_l(s^2+\omega_{\rm Ar}^2) - m_r(s^2+\omega_{\rm Al}^2)\right]F_2(s)}{(m_l+m_r)\left[s^2+\omega_{\rm Al}^2 - \frac{m_l}{m_l+m_r}(\omega_{\rm Al}^2-\omega_{\rm Ar}^2)\right]} \quad (A.14)$$

$$I_5 = -\frac{1}{2\pi i}\int_C F_5(s)ds, \quad (A.15)$$

with

$$F_5(s) = \frac{\left[m_l(s^2+\omega_{\rm Ar}^2) - \frac{m_r^2}{m_l}(s^2+\omega_{\rm Al}^2)\right]F_1(s)}{(m_l+m_r)\left[s^2+\omega_{\rm Al}^2 - \frac{m_l}{m_l+m_r}(\omega_{\rm Al}^2-\omega_{\rm Ar}^2)\right]} \quad (A.16)$$

and

$$I_6 = \frac{1}{2\pi i}\int_C F_6(s)ds, \quad (A.17)$$

with

$$F_6(s) = \frac{m_l\, m_r^2\, F_1(s)}{(m_l+m_r)\left[s^2+\omega_{\rm Al}^2 - \frac{m_l}{m_l+m_r}(\omega_{\rm Al}^2-\omega_{\rm Ar}^2)\right]} \times \left(\frac{s^2c_{\rm Sr}^2}{s^2+\omega_{\rm Sr}^2} - \frac{s^2c_{\rm Sl}^2}{s^2+\omega_{\rm Sl}^2}\right). \quad (A.18)$$

To evaluate the integral I_3, we note that $F_3(s)$ has one pole at $s = 0$ (see Eq. A4 for $F_1(s)$) and two poles at $s = \pm i\omega$. In the latter case, the denominator of $F_3(s)$ can be written as

$$\omega^2 = \omega_{\rm Al}^2 - \frac{n_l}{n_l + n_r}(\omega_{\rm Al}^2 - \omega_{\rm Ar}^2), \tag{A.19}$$

which is the dispersion relation for MHD surface waves (see Eq. 41) and $n_{l,r}$ is given by Eq. (42). Calculating the residues of $F_3(s)$ at $s = 0$ and $s = \pm i\omega$, we obtain

$$\text{Res } F_3(s)|_{\rm s=o} = \frac{\omega_{\rm Ar}^2 - \omega_{\rm Al}^2}{\omega_{\rm Ar}^2 + \omega_{\rm Ar}^2} e^{k(x-x')} \tag{A.20}$$

and

$$\text{Res } F_3(s)|_{\rm s=\pm i\omega} = -\frac{1}{2}\frac{k}{n_r}\frac{n_l(\omega_{\rm Ar}^2 - \omega^2) - n_r(\omega_{\rm Al}^2 - \omega^2)}{(n_l + n_r)\omega^2} \times e^{-n_r x'} e^{n_l x} e^{\pm i\omega t}. \tag{A.21}$$

By adding these three residues and multiplying them by $2\pi i$, we get

$$I_3 = -\frac{Q}{2}\frac{k}{n_r}\frac{n_l(\omega_{\rm Ar}^2 - \omega^2) - n_r(\omega_{\rm Al}^2 - \omega^2)}{(n_l + n_r)\omega^2}\, e^{-n_r x'} e^{n_l x} \times \cos(\omega t) \; + \; \frac{Q}{2}\frac{\omega_{\rm Ar}^2 - \omega_{\rm Al}^2}{\omega_{\rm Ar}^2 + \omega_{\rm Ar}^2} e^{k(x-x)}. \tag{A.22}$$

Now, we consider the integral I_4. Since the poles at $s = \pm i\omega$ are the same as for $F_3(s)$, we can use Eq. (A21) to write

$$\text{Res } F_4(s)|_{\rm s=+i\omega} + \text{Res } F_4(s)|_{\rm s=-i\omega} = \frac{k}{n_r}\left(\frac{c_{\rm Sr}^2}{c_{\rm Sr}^2 + c_{\rm Ar}^2}\right) \times \frac{n_l(\omega_{\rm Ar}^2 - \omega^2) - n_r(\omega_{\rm Al}^2 - \omega^2)}{(n_l + n_r)(\omega_{\rm Tr}^2 - \omega^2)} e^{-n_r x'} e^{n_l x} \cos(\omega t). \tag{A.23}$$

There are two more poles at $s = \pm i\omega_{\rm Tr}$, however, at these two poles $m_r \to \infty$. Since the latter is not physical, we take $m_{l,r} = n_{l,r}$ (see discussion following Eq. A7) and obtain

$$\text{Res } F_4(s)|_{\rm s=+i\omega_{Tr}} + \text{Res } F_4(s)|_{\rm s=-i\omega_{Tr}} = \frac{k}{n_r}\left(\frac{c_{\rm Sr}^2}{c_{\rm Sr}^2 + c_{\rm Ar}^2}\right) \times \frac{n_l(\omega_{\rm Ar}^2 - \omega_{\rm Tr}^2) - n_r(\omega_{\rm Al}^2 - \omega_{\rm Tr}^2)}{(n_l + n_r)(\omega_{\rm Tr}^2 - \omega^2)} e^{-n_r x'} e^{n_l x} \times \cos(\omega_{\rm Tr} t). \tag{A.24}$$

Thus, we have

$$I_4 = -\frac{Q}{2}\frac{k}{n_r}\left[\frac{n_l(\omega_{\rm Ar}^2 - \omega^2) - n_r(\omega_{\rm Al}^2 - \omega^2)}{(n_l + n_r)(\omega_{\rm Tr}^2 - \omega^2)}\cos(\omega_{\rm Tr}) + \frac{n_l(\omega_{\rm Ar}^2 - \omega_{\rm Tr}^2) - n_r(\omega_{\rm Al}^2 - \omega_{\rm Tr}^2)}{(n_l + n_r)(\omega_{\rm Tr}^2 - \omega^2)}\cos(\omega_{\rm Tr} t)\right] \times \left(\frac{c_{\rm Sr}^2}{c_{\rm Sr}^2 + c_{\rm Ar}^2}\right) e^{-n_r x'} e^{n_l x}. \tag{A.25}$$

The next integral to be evaluated is I_5. The form of the function $F_5(s)$ is slightly different than $F_3(s)$ but the poles are the same, namely, $s = 0$ $s = \pm i\omega$. Calculating the residues at these poles, we find

$$\text{Res } F_5(s)|_{\rm s=o} = \frac{\omega_{\rm Ar}^2 - \omega_{\rm Al}^2}{\omega_{\rm Ar}^2 + \omega_{\rm Ar}^2} e^{k(x-x')}, \tag{A.26}$$

and

$$\text{Res } F_5(s)|_{\rm s=\pm i\omega} = -\frac{1}{2}\frac{k}{n_r}\frac{n_l^2(\omega_{\rm Ar}^2 - \omega^2) - n_r^2(\omega_{\rm Al}^2 - \omega^2)}{n_l(n_l + n_r)\omega^2} \times e^{-n_r x'} e^{n_l x} e^{\pm i\omega t}. \tag{A.27}$$

Thus, we can write

$$I_5 = -\frac{Q}{2}\frac{k}{n_r}\frac{n_l^2(\omega_{\rm Ar}^2 - \omega^2) - n_r^2(\omega_{\rm Al}^2 - \omega^2)}{n_l(n_l + n_r)\omega^2}\, e^{-n_r x'} e^{n_l x} \times \cos(\omega t) \; + \; \frac{Q}{2}\frac{\omega_{\rm Ar}^2 - \omega_{\rm Al}^2}{\omega_{\rm Ar}^2 + \omega_{\rm Ar}^2} e^{k(x-x)}. \tag{A.28}$$

According to Eq. (A10), the last integral to be evaluated is I_6. The integrand $F_6(s)$ has two poles at $s = \pm i\omega$, which give

$$\text{Res } F_6(s)|_{\rm s=+i\omega} + \text{Res } F_6(s)|_{\rm s=-i\omega} = \frac{k n_l n_r}{n_l + n_r} \times \left(\frac{c_{\rm Sr}^2}{\omega_{\rm Sr}^2 - \omega^2} - \frac{c_{\rm Sl}^2}{\omega_{\rm Sl}^2 - \omega^2}\right) e^{-n_r x'} e^{n_l x}. \tag{A.29}$$

There are four additional poles at $s = \pm i\omega_{\rm Sr}$ and $s = \pm i\omega_{\rm Sl}$, which give $m_r = 0$ and $m_l = 0$, and Res $F_6(s) = 0$. Formally, in our approach $m_r > 0$ and $m_l > 0$, which means that the poles should not be taken into account in the evaluation of this integral. Either way, there is no contribution from these poles to the integral I_6. Thus, we can write

$$I_6 = \frac{Q}{2}\frac{k n_l n_r}{n_l + n_r}\left(\frac{c_{\rm Sr}^2}{\omega_{\rm Sr}^2 - \omega^2} - \frac{c_{\rm Sl}^2}{\omega_{\rm Sl}^2 - \omega^2}\right) e^{-n_r x'} e^{n_l x} \times \cos(\omega t). \tag{A.30}$$

After evaluating the integrals I_3, I_4, I_5 and I_6 (see Eqs. A22, A25, A28 and A30, respectively), we may add them up to obtain the integral given by Eq. (A10).

Finally, we have to evaluate the integral with the coefficient $C_6(s)$ in Eq. (A1). This is easy because the form of $C_6(s)$ is simple (see Eq. 27 in the main text). The result is

$$I_7 = \frac{1}{2\pi i}\int_C C_6(s) e^{k(x-x')} e^{st} ds = -Q/2 e^{k(x-x')}. \tag{A.31}$$

Having evaluated all integrals in Eq. (A1), we may now obtain the inverse Laplace transform for $\overline{u_l}(x, s)$ by adding the integrals I_1 through I_7. After performing some algebraic manipulations and defining

$$\alpha_0 = \frac{k}{n_r}\frac{c_{\rm Sr}^2}{c_{\rm Sr}^2 + c_{\rm Ar}^2}\,, \tag{A.32}$$

$$\alpha_1 = \frac{n_l(\omega_{\rm Ar}^2 - \omega_{\rm Tr}^2) - n_r(\omega_{\rm Al}^2 - \omega_{\rm Tr}^2)}{(n_l + n_r)\,(\omega_{\rm Tr}^2 - \omega^2)}\,\alpha_0\,, \tag{A.33}$$

$$\alpha_2 = \frac{n_l(\omega_{\rm Ar}^2 - \omega^2) - n_r(\omega_{\rm Al}^2 - \omega^2)}{(n_l + n_r)\,(\omega_{\rm Tr}^2 - \omega^2)}\,\alpha_0\,, \tag{A.34}$$

and

$$\alpha_3 = \frac{k}{n_r}\left(\frac{n_r}{n_l + n_r}\right)\left[\left(1 - \frac{n_r}{n_l}\right)\left(\frac{\omega_{\rm Al}^2 - \omega^2}{\omega^2}\right) + \left(\frac{n_l n_r c_{\rm Sr}^2}{\omega_{\rm Sr^2} - \omega^2} - \frac{n_l n_r c_{\rm Sl}^2}{\omega_{\rm Sl^2} - \omega^2}\right)\right]\,, \tag{A.35}$$

we obtain

$$u_l(x,t) = \frac{Q}{2}\left[(\alpha_1 - \alpha_0)\,\cos(\omega_{\rm Tr}t) + (\alpha_3 - \alpha_2)\,\cos(\omega t)\,\right]\,e^{n_l x}e^{-n_r x'}\,, \tag{A.36}$$

which is the same as Eq. (44) in the main text. The same procedure can now be used to obtain the inverse Laplace transform for $u_{r1}(x,t)$ and $u_{r2}(x,t)$.

References

Cally P.C., 1985, Aust. J. Phys. 38, 825
Chen L., Hasegawa A., 1974, Phys. Fluids 17, 1399
Davila J.M., 1987, ApJ 317, 514
Goossens M., 1991, In: Ulmschneider P., Priest E.R., Rosner R. (eds.) Mechanism of Chromospheric and Coronal Heating Springer-Verlag, Berlin, p. 480
Goossens M., 1994, Space Sci. Rev. 68, 51
Hollweg J.V., 1985, In: Buti B. (ed.) Advances in Space Plasma Physics. World Scientific Publ., Singapore, p. 77
Huang P., 1995, Ph.D. Thesis, Univ. of Alabama in Huntsville
Huang P., 1996, Phys. Plasmas 3, 2579
Huang P., Musielak Z.E., Ulmschneider P., 1999, Astron. Astrophys. 342, 300
Ionson J.A., 1978, ApJ 226, 650
Kieras C.E., Tataronis J.A., 1982, Phys. Fluids 25, 1228
Lanzerotti L.J., Southwood D.J., 1979, In: Kennel C.F., Lanzerotti L.J., Parker E.N. (eds.) Solar System Plasma Physics. North-Holland, New York, p. 109
Lee M.A., Roberts B., 1986, ApJ 301, 430
Narain U., Ulmschneider P., 1990, Space Sci. Rev. 54, 377
Narain U., Ulmschneider P., 1996, Space Sci. Rev. 75, 453
Ofman L., Davila J.M., Steinolfson R.M., 1994, Geophys. Res. Let. 21, 2259
Roberts B., 1981, Sol. Phys. 69, 27
Roberts B., 1991, In: Priest E.R., Hood A.W. (eds.) Advances in Solar Solar System Magnetohydrodynamics. Cambridge Univ. Press, Cambridge, p. 105
Roberts B., Webb A.R., 1978, Solar Phys. 56, 5
Solanki S.K., 1993, Space Sci. Rev. 63, 1
Takahashi K., McPherron R.L., 1984, Space Sci. Rev. 35, 301
Tataronis J.A., Grossmann W., 1973, Z. Phys. 261, 203
Tataronis J.A., Lewis H.R., 1986, Phys. Fluids 29, 167
Wentzel D.G., 1979, ApJ 227, 319
Wu S.T., Xiao Y.C., Musielak Z.E., Suess S.T., 1996, Solar Phys. 163, 291
Xiao Y.C., 1989, Ph.D. Thesis, Univ. of Alabama in Huntsville